Published in final edited form as:
Immunity. 2014 January 16; 40(1): 91–104. doi:10.1016/j.immuni.2013.11.019.

Embryonic and adult-derived resident cardiac macrophages are maintained through distinct mechanisms at steady state and during inflammation

Slava Epelman[1], **Kory J. Lavine**[1], **Anna E. Beaudin**[2], **Dorothy K. Sojka**[3], **Javier A. Carrero**[4], **Boris Calderon**[4], **Thaddeus Brija**[1], **Emmanuel L. Gautier**[4], **Stoyan Ivanov**[4], **Ansuman T. Satpathy**[4], **Joel D. Schilling**[4,5], **Reto Schwendener**[6], **Ismail Sergin**[1], **Babak Razani**[1], **E. Camilla Forsberg**[2], **Wayne Yokoyama**[3], **Emil R. Unanue**[4], **Marco Colonna**[4], **Gwendalyn J. Randolph**[1,4], and **Douglas L. Mann**[1,7]

[1]Center for Cardiovascular Research, Division of Cardiology, Dept. of Medicine, Washington University School of Medicine, St. Louis, MO. 63110. USA [2]Dept. of Biomolecular Engineering, Baskin School of Engineering, University of California, Santa Cruz, Santa Cruz CA. 95064. USA [3]Division of Rheumatology, Washington University School of Medicine. 63110. USA [4]Dept. of Pathology and Immunology, Washington University School of Medicine. 63110. USA [5]Diabetic Cardiovascular Disease Center, Washington University School of Medicine. 63110. USA [6]Institute of Molecular Cancer Research, University Zurich, CH-8057 Zurich, Switzerland

Summary

Cardiac macrophages are crucial for tissue repair after cardiac injury but have not been well characterized. Here we identify four populations of cardiac macrophages. At steady state, resident macrophages were primarily maintained through local proliferation. However, after macrophage depletion or during cardiac inflammation, Ly6c^{hi} monocytes contributed to all four macrophage populations, whereas resident macrophages also expanded numerically through proliferation. Genetic fate mapping revealed that yolk-sac and fetal monocyte progenitors gave rise to the majority of cardiac macrophages, and the heart was among a minority of organs in which substantial numbers of yolk-sac macrophages persisted in adulthood. CCR2 expression and dependence distinguished cardiac macrophages of adult monocyte versus embryonic origin. Transcriptional and functional data revealed that monocyte-derived macrophages coordinate cardiac inflammation, while playing redundant but lesser roles in antigen sampling and efferocytosis. These data highlight the presence of multiple cardiac macrophage subsets, with different functions, origins and strategies to regulate compartment.

[7]Corresponding Author: Douglas L. Mann, MD, Cardiovascular Division, Campus Box 8086, 660 South Euclid Avenue, St. Louis, MO 63110-1093, Phone: (314) 362-8908, FAX: (314) 454-5550, dmann@dom.wustl.edu.

Supplemental Information
Includes detailed information on each experiments performed in the supplemental experimental procedures, seven figures and three tables.

Keywords

Macrophage; Cardiac; Inflammation; Angiotensin II; Yolk Sac

Introduction

Cardiovascular disease is the leading cause of adult mortality in the developed world and continues to be a major burden to health care systems. Whether through acute ischemic injury or through the gradual impairment of cardiac function secondary to a variety of clinical pathologies, release of neurohormonal mediators such as angiotensin II (AngII), ultimately leads to irreversible heart failure (Francis, 2011). Data both from both animal models and clinical studies show that after cardiac injury mononuclear phagocytes (MNPs), including monocytes, macrophages and dendritic cells (DCs), expand within the myocardium. In a context-dependent manner, these cells modulate (either enhance or suppress) the ability of myocardial tissue to recover after injury. Interestingly, both increased or insufficient macrophage expansion impairs infarct healing, however the exact cell types that may promote injury or enhance tissue regeneration are not know (Nahrendorf et al., 2007; Panizzi et al., 2010).

At steady-state, the traditional view has been that tissue macrophages arise from circulating blood monocytes. Recent studies have demonstrated that tissue macrophages such as microglia, Kupffer cells and Langerhans cells are established prenatally, arise independent of the hematopoietic transcription factor Myb and persist into adulthood (Ginhoux et al., 2010; Yona et al., 2013; Schulz et al., 2012). Fate mapping studies using the pan macrophage marker CX3CR1 confirm the prenatal development of macrophages in many, but not all tissues, with the notable exception being intestinal CX3CR1^{+} macrophages, which are continually replenished by blood Ly6c^{hi} monocytes (Zigmond et al., 2012). In addition, it is also becoming apparent that tissue resident macrophages are maintained and can expand dramatically by *in situ* proliferation, rather than recruitment of blood monocytes (Davies et al., 2013; Jenkins et al., 2011). Such rigorous analysis has not yet been applied to the myocardium. Currently, it is not known what the relationship is between blood monocytes and cardiac macrophages, and which, if any, cardiac macrophage populations are established prenatally. Moreover, how these populations change during cardiac stress and what functions are possessed by individual subsets has not been unexplored.

Here we characterized cardiac monocytes and macrophages within the myocardium both at steady state and after cardiac stress. By using complementary *in vivo* cell tracking, parabiosis, bone marrow transplants and fate mapping studies, we found the majority of cardiac macrophages were established prior to birth, with significant contribution from yolk sac progenitors. The adult mammalian heart contained specific subsets of both embryonic and adult derived macrophages, which were maintained through local proliferation and replacement by blood monocytes, respectively (see summary Fig S7). Following the disruption of homeostasis, both within the myocardium and other organs, blood monocyte-derived macrophages were not only recruited, but permanently replaced embryonically established resident macrophage populations. Transcriptional analysis of resident cardiac macrophages revealed that monocytederived macrophages coordinate cardiac inflammation, while playing redundant but lesser roles in antigen sampling and efferocytosis

Results

The adult heart contains distinct cardiac macrophage subsets

We devised a gating strategy in order to differentiate cardiac macrophages from other immune cells in the myocardium. In addition to cell surface markers, we took advantage of the autofluorescent (Auto) properties of cardiac macrophages in our gating strategy (Fig 1A, and full strategy in Fig S1A). The majority of $CD45^+$ cells in the myocardium were $F4/80^+CD11b^+$, and within this heterogeneous population, we found four macrophage subsets. The primary cardiac macrophage populations were $Auto^+Ly6c^-$ and either MHC-II^{hi} or MHC-II^{lo} (R1 or R2 - Fig 1A, respectively). Their macrophage identity was confirmed using the highly specific macrophage markers MerTK and (Fig 1B) (Gautier et al., 2012). MHC-II^{Hi} macrophages were $CX3CR1^{Hi}$, $CD206^{int}$ and contained a small subset that was $CD11c^{hi}$, suggesting additional heterogeneity, while MHC-II^{lo} macrophages were $CX3CR1^{int}$, $CD206^{hi}$ and $CD11c^{lo}$ (Fig 1B). We identified a third macrophage population that retained Ly6c expression and represented ∼2% of total cardiac macrophages (Fig 1A, R3). Monocytes (R4) were found in the $Auto^-$ gate, and could be separated from $Ly6c^+$ macrophages (R3) by a lack of MerTK and CD206 expression (Fig 1B). To confirm that these macrophage populations were in the tissue, we injected anti-CD45 *i.v.* immediately before harvest to label all blood leukocytes (Tagliani et al., 2011). Cardiac macrophages did not label with *i.v.* anti-CD45, while neutrophils, B cells and a high proportion of $Ly6c^{Hi}$ monocytes were labeled, indicating these cells were in the microvasculature (Fig 1C). Both of the main $Ly6c^-$ macrophage populations (R1 & R2) were larger, more granular and expressed higher amounts of F4/80 than cardiac monocytes (Fig S1A).

To ensure our macrophage populations were pure we needed to adequately account for cardiac DCs. The largest pool of DCs (representing ∼1% of total $CD45^+$ cells, R5), were found primarily in the $Auto^-$ gate and were either $CD103^+CD11b^-$ (R6) or $CD103^-CD11b^{hi}$ (R7, Fig 1D). Both DC subsets expressed high amounts of the classic DC transcription factor Zbtb46 (Fig 1D) (Satpathy et al., 2012). As $CD11b^+$ DCs can be difficult to distinguish from macrophages, we determined where these cells appeared in macrophage our gating strategy (Hashimoto et al., 2011). By gating on $CD11b^+Zbtb46^{hi}$ DCs, we found that $CD11b^+$ DCs were $F4/80^-$, and thus fell outside of the macrophage gates (Fig S1B). While MHC-II^{hi} macrophages (R1) contained $CD11c^+$ cells (5–15%), only a small fraction were $CD103^+$ DCs, and after excluding these $CD103^+$ DCs, the macrophage identity of the remaining R1-$CD11c^{hi}$ subset was confirmed by MerTK expression, consistent with a new fourth cardiac macrophage population (Fig 1E). All cardiac macrophage gates had negligible Zbtb46 signal, confirming that DCs were not significantly contaminating any of our macrophage populations (Fig 1F). We have therefore identified four macrophage subsets in the adult heart (Fig S7B) during steady state, revealing a previously unknown heterogeneity.

Distinct mechanisms regulate cardiac macrophage turnover in steady and following the disruption of homeostasis

To determine whether turnover of resident macrophages occurred through replacement by blood monocytes, we created parabiotic mice that differed only by expression of CD45.1 and CD45.2. Blood $Ly6c^{hi}$ monocytes achieved ∼30% chimerism over 14 days, which was mirrored by cardiac $Ly6c^{hi}$ monocytes (Fig 2A). After normalizing to blood monocyte chimerism, we found there was very little replacement of the MHC-II^{hi} or MHC-II^{lo} $CD11c^{lo}$ macrophages, and only modest replacement of $CD11c^{hi}$ MHC-II^{hi} macrophages (R1-$CD11c^{hi}$) by chimeric peripheral monocytes, suggesting these populations were either locally derived and/or long lived (Fig 2A). $Ly6c^+$ macrophages (R3) had some, but not complete replacement by monocytes. To confirm these findings we adoptively transferred $CD150^+$ fetal liver hematopoietic stem cells (HSCs) into animals that were sublethally

irradiated in order to reduce, but not extinguish the resident macrophage populations (Hashimoto et al., 2013). When engraftment was assessed 16 weeks later we again found that the CD11c^{lo} macrophage populations (R1 and R2) had significantly reduced engraftment rates compared to the other populations suggesting these macrophage populations largely persist independent of blood monocyte input (Fig 2B).

To further investigate the mechanisms by which cardiac macrophage populations were replenished we depleted cardiac monocytes / macrophages with a single *i.v.* injection of clodronate liposomes. We observed a profound depletion of resident macrophage populations, with a corresponding expansion of Ly6c^{+} monocytes and neutrophils, which began to decline once macrophages repopulated the myocardium (Fig 2C). To assess the role of blood monocytes in replenishing these macrophage subsets, we labeled blood Ly6c^{Hi} monocytes *in vivo* with fluorescents beads (Tacke et al., 2006) (Fig 2D). Following macrophage depletion, the percentage of bead^{+} cells increased in all macrophage compartments suggesting that blood Ly6c^{hi} monocytes can differentiate into all macrophage subsets (Fig 2E). In addition, we wondered if resident macrophages proliferated following depletion. To answer this question, we pulsed animals with BrdU 2 hrs prior to harvest to label proliferating cardiac macrophages. In this time frame, proliferating Ly6c^{Hi} monocytes remain in the bone marrow and have not been released into circulation (Fig 2F). Following depletion, an increased rate of proliferation was detected in all macrophage populations except Ly6c^{+} macrophages (Fig 2G). Together, these data argue that resident CD11c^{lo} MHC-II^{hi} and MHC-II^{lo} macrophages exist separate from blood monocytes during the steady state and are renewed through *in situ* proliferation. When homeostasis was disrupted following macrophage depletion, Ly6c^{hi} monocytes have the capacity to readily differentiate into these macrophage compartments. In contrast, CD11c^{hi} MHC-II^{hi} macrophages and Ly6c^{+} macrophages appear to be replenished through both local expansion and monocyte replacement to differing degrees.

Peripheral Ly6c^{hi} monocyte recruitment and local proliferation drive cardiac macrophage expansion during stress

The angiotensin II (AngII) pathway represents a clinically relevant, evolutionary conserved pathological neurohormonal signaling cascade central to virtually all forms of cardiovascular disease (Francis, 2011). Therefore, we sought to explore the inflammatory effects of AngII on cardiac macrophage populations. AngII induced the rapid influx of Ly6c^{hu} monocytes and subsequent expansion of CD11c^{lo} MHC-II^{lo} (R2) and Ly6c^{+} macrophages (R3) (Fig 3A, and Fig S2A-time course). AngII induced the expansion of CD11c^{hi} MHC-II^{hi} macrophages (R1-CD11c^{hi}) and a decrease of CD11c^{lo} MHC-II^{hi} macrophages highlighting the dynamic relationship of cardiac macrophages subsets during stress. MerTK and CD64 labeling confirmed the expanded CD11c^{lo} MHC-II^{lo} subset were macrophages (Fig S2B), as were the remaining CD11c^{lo} MHC-II^{hi} macrophages (data not shown). Similar expansion of macrophages was observed after myocardial infarction (Fig S2C). Consistent with AngII as an inflammatory stimulus, Ly6c^{hi} blood monocytes from mice that received AngII upregulated TLR4 and MD-2, and when stimulated with the TLR4 agonist (LPS), produced higher amounts of TNF-α (Fig S2D – S2E), suggesting peripheral activation occurred prior to infiltration. Thus, the AngII infusion model proved to be a useful system to investigate macrophage dynamics during cardiac stress.

To determine which subset of blood monocytes (if any) gave rise to cardiac macrophages after AngII infusion we used the monocyte tracking system described previously, in which fluorescent beads were preferentially phagocytosed by either Ly6c^{hi} or Ly6c^{lo} peripheral blood monocytes (Fig S2F). When Ly6c^{lo} blood monocytes were bead-labeled, there was no enrichment of bead^{+} cells in cardiac macrophages in response to AngII infusion, whereas

bead^{+} blood Ly6c^{hu} monocytes gave rise to all macrophage populations (Fig 3B). To confirm these findings, we took advantage of the fact that Ly6c^{Hi} monocytes preferentially take up BrdU compared to Ly6c^{lo} monocytes due to their high rate of production and release from the bone marrow (Zhu et al., 2009). After a 2 day BrdU pulse, ∼40% of Ly6c^{hi} blood monocytes were labeled. Similarly, there was enrichment of BrdU-labeled cells in all macrophage compartments after AngII infusion (Fig 3C). We confirmed that the progeny of monocytes entered into all macrophage subsets by initially gating on either all cardiac bead^{+} or BrdU^{+} cells and then tracked their contribution to resident macrophage compartments (Fig S2G).

It has become apparent that in addition to monocyte recruitment, macrophages are maintained through local proliferation (Jenkins et al., 2011; Davies et al., 2013). To assess the effect of AngII on local macrophage proliferation we analyzed expression of Ki-67, a nuclear protein expressed by proliferating cells. At steady-state, a relatively high percentage of CD11c^{-}MHC-II^{hi} and MHC-II^{lo} macrophages were Ki-67^{+} (18% ± 2% and 26%±2%, respectively), which increased with AngII infusion (Fig 3D). We then quantified macrophages in S-phase specifically using a 2 hr BrdU pulse and again found AngII induced proliferation of all macrophage subsets (Fig 3E). Thus cardiac macrophage cell numbers increase during inflammation through both recruitment of blood Ly6c^{+} monocytes and *in situ* proliferation. Given that monocytes contribute to all macrophage populations during inflammation, it is not possible to separate recruitment from local expansion using cell surface markers alone.

CCR2 deficient mice distinguish local macrophage expansion from peripheral monocyte influx

To separate the contribution of infiltrating Ly6c^{hi} monocytes from locally expanding resident cardiac macrophages to the expansion of macrophage cell numbers we examined CCR2- deficient (*Ccr2*$^{GFP/GFP}$) mice, which lack peripheral blood Ly6c^{hi} monocytes (Fig S3A) (Serbina and Pamer, 2006). During our initial characterization of the *Ccr2*$^{GFP/+}$ mice, we found cardiac monocytes (R4) were CCR2^{+} while CD11c^{Low} (R1 and R2), and Ly6c^{+} (R3) macrophages were CCR2^{-} (Fig 4A). CD11c^{hi} MHC-II^{hi} macrophages (R1- CD11c^{Hi}) were largely CCR2^{+}, allowing us to more easily distinguish the two MHC-II^{hi} macrophage populations (Fig 4A–4B). Consistent with tissue identity, these CCR2^{+} macrophages were located within the myocardium and were MerTK^{+} CD64^{+} CD11c^{hi} CD206^{+} (R8, Fig 4B–4C).

We then compared macrophage numbers during at steady state and following after AngII infusion in *Ccr2CR2* $^{GFP/+}$ (blood Ly6c^{Hi} monocyte sufficient) to *Ccr2CR2* $^{GFP/GFP}$ (blood Ly6c^{hi} monocyte deficient) mice. We examined cardiac CCR2^{+} and CCR2^{-} compartments specifically because they allowed us to determine ability of these populations to regulate macrophage compartment size. In the steady state, cardiac CCR2^{+} macrophages were reduced (R8) in *Ccr2*$^{GFP/GFP}$ mice, while CCR2^{-} populations had a normal distribution of CD11c^{lo} MHC-II^{hi} and MHC-II^{lo} macrophages, consistent with their independence from blood monocytes (Fig 4D–4E). After AngII infusion, CCR2^{+} MHC-II^{hi} macrophages and CCR2^{+} Ly6c^{hi} monocyte (R4) numbers increased, in *Ccr2*$^{GFP/+}$ mice but not *Ccr2*$^{GFP/GFP}$ mice (Fig 4D–4E)). CCR2^{-}MHC-II^{hi} macrophages (R1) were rapidly lost during AngII infusion, which was similar between *Ccr2*$^{GFP/+}$ and *Ccr2*$^{GFP/GFP}$ mice, and was identical to the loss of CD11c^{lo} MHC-II^{hi} macrophages we previously observed (Fig 3A).

MHC-II^{lo} CCR2^{-} macrophages (R2) had the largest numerical expansion after AngII infusion, and our data suggest expansion occurred through at least two mechanisms. The first was *in situ* proliferation of resident macrophages. This conclusion was supported by the fact that this compartment expanded in the absence of peripheral monocytes (*Ccr2*$^{GFP/GFP}$

mice, Fig 4D–4E) and the percentage of macrophages in cell cycle and absolute number of macrophages in cell cycle (S-phase, $BrdU^+$) were identical in the absence of peripheral monocytes (*Ccr2*$^{GFP/GFP}$ mice, Fig 4F–4G). The second mechanism involved the recruitment of $CCR2^+$ monocytes that downregulated CCR2 and became $CCR2^-$ MHC-II^{lo} $Ly6c^-$ macrophages. This conclusion was supported by the fact that blood $Ly6c^{hi}$ monocytes entered that compartment after AngII infusion (Fig 3B–3C), and when $Ly6c^{hi}$ monocytes were absent (*Ccr2*$^{GFP/GFP}$ mice), the expansion of this compartment was in part blunted (Fig 4D–4E). Lastly, there was a small expansion of $Ly6c^+$ macrophages with AngII, which was comprised of mixed populations of $CCR2^+$ and $CCR2^-$ macrophages, and was dependent on blood monocytes (lost in *Ccr2*$^{GFP/GFP}$ mice, data not shown).

Similarly, depletion of cardiac macrophages using clodronate liposomes induced a robust increase in $CCR2^+$ MHC-II^{hi} macrophages numbers during the re-expansion phase which was reduced in *Ccr2*$^{GFP/GFP}$ animals (Fig S3B–S3C). Repopulation of $CCR2^-$ macrophages (both MHC-II^{hi} and MHC-II^{lo}) was unchanged in the absence of monocyte recruitment. Together, these data revealed that resident cardiac macrophages ($CCR2^-$ $CD11c^{lo}$ $Ly6c^-$) expanded without monocyte input through *in situ* proliferation, while monocytes that expressed CCR2, were able to contribute to both $CCR2^+$ and $CCR2^-$ macrophages subsets through recruitment, and subsequent proliferation.

Adult cardiac macrophages are established during embryonic development

Recent studies have indicated that many tissue-resident adult macrophages are established embryonically and persist separate from the blood monocyte pool (Schulz et al., 2012; Yona et al., 2013; Hoeffel et al., 2012). However, the ontological origin of cardiac macrophages has yet to be explored. Embryonic macrophage populations are established during two phases. Primitive hematopoiesis occurs during early development (E7.5-E11.5), where embryonic yolk sac progenitors develop into either yolk-sac macrophages or red blood cells (Lichanska and Hume, 2000). Later macrophage populations (E11.5 – E16.5) arise from fetal liver HSCs through definitive hematopoiesis, which gives rise to all immune lineages, including monocyte-derived macrophages (Kumaravelu et al., 2002; Yona et al., 2013; Hoeffel et al., 2012). Adult brain microglia originate strictly from yolk-sac macrophages (Ginhoux et al., 2010), and while the initial characterization of yolk sac-derived macrophages suggested a broad persistence of this subset in multiple organs after birth (Schulz et al., 2012), subsequent studies have indicated that fetal liver monocytes may be the primary source at least for skin Langerhans cells and alveolar macrophages, suggesting that the origins of tissue macrophages may be more complex (Hoeffel et al., 2012; Guilliams et al., 2013). To explore the origin of resident cardiac macrophages we undertook several complimentary approaches.

Primitive macrophages seeded the early embryonic heart by ∼E9.5 (data not shown) and could be easily detected by ∼E10.5 (Fig 5A). These early macrophages were yolk sac-derived since they appeared in the heart prior to fetal liver hematopoiesis (Hoeffel et al., 2012). Yolk sacderived macrophages were MHC-II^{lo}, $CX3CR1^{hi}$ and had the characteristic $F4/80^{hi}$ $CD11b^{lo}$ expression pattern observed on embryonic yolk sac macrophages in many tissues (Fig 5B) (Schulz et al., 2012). From ∼E12.5-E16.5 we observed the appearance of a second $CX3CR1^{lo}$ macrophage wave, which had the fetal liver monocyte derived pattern of $F4/80^{lo}$ $CD11b^{hi}$ in the heart, lung, yolk sac (Fig 5B) and kidney (data not shown). In contrast to the other tissues, where $CX3CR1^{hi}$ and $CX3CR1^{lo}$ macrophages partitioned well using differential expression of F4/80 and CD11b, cardiac macrophages were universally $F4/80^{lo}$ $CD11b^{hi}$ (Fig 5B), thus indicating a more formal genetic fate mapping approach would be required to define their ontological origin during development and facilitate analyses of these populations in adulthood.

Self-renewing, adult definitive HSCs transiently upregulate FLT3 as they differentiate into all hematopoietic lineages (Boyer et al., 2011). By crossing *Flt3*-Cre mice to *Rosa*-mTmG reporter mice we were able to track cells that either did (*Flt*-Cre^{+}) or did not (*Flt3*-Cre^{-}) pass through a FLT3^{+} stage and could differentiate definitive HSC-derived macrophages from those that developed independently of HSC (such as from embryonic yolk sac progenitor or via other, fetal FLT3-independent pathways). To determine which embryonic macrophages were derived from HSCs we analyzed *Flt3*-Cre *x Rosa* mTmG reporter mice at E14.5, a time point at which definitive hematopoiesis has been established in the fetal liver. We found that all F4/80^{hi}CD11b^{lo} (phenotypically yolk sac-derived) macrophages were entirely FLT3-Cre^{-}, while macrophages thought to be derived from fetal liver monocytes (F4/80^{lo}CD11b^{hi}) contained a relatively small population of *Flt3*-Cre^{+} (∼5%) macrophages in all organs tested, suggesting that infiltration of HSC-derived monocytes had begun (Fig 5C). Recombination rates driven by FLT3 were surprising low during embryonic development, but by 4 weeks of age, recombination had reached ∼85–95% in blood monocytes (data now shown). We then followed *Flt3*-Cre^{-} cardiac macrophages over time and demonstrated that they persisted in large numbers in adult mice (20 weeks old) (Fig 5D). We found that only CD11c^{+}CCR2^{+} macrophages were primarily derived from HSC precursors (*Flt3*-Cre^{+}), while the main MHC-II^{hi} and MHC-II^{lo} macrophage subsets (CD11c^{lo}CCR2^{-}Ly6c^{-}), and Ly6c^{+} macrophages originated from *Flt3*-Cre^{-} pathways (Fig 5D). Comparison of cardiac macrophages to other tissue macrophages demonstrated that with the exception of brain microglia, which were entirely *Flt3*-Cre^{-}, most adult tissue resident macrophage compartments contained populations with both *Flt3*-Cre^{+} and *Flt3*-Cre^{-} subsets (Fig 5D).

The heart is one of the few adult organs that retained yolk-sac macrophages in significant numbers

Given the low recombination rates in the embryo, we could not be sure if in the adult, *Flt3*-Cre^{-} resident macrophages were truly FLT3-independent and originated from yolk sac macrophages (derived outside HSCs), or whether they originated from HSC-dependent fetal liver monocyte pathways. Even if derived from fetal liver monocytes, *Flt3*-Cre^{-} cardiac macrophages were not replaced by *Flt3*-Cre^{+} blood monocytes in adult animals. To more definitively address this issue we labeled yolk sac-derived macrophages by administering tamoxifen at E8.5 in *CD115-Mer-iCre-Mer* x *Rosa* mTmG mice (Qian et al., 2011; Schulz et al., 2012). Approximately ∼30% of macrophages within the E10.5 yolk sac were labeled by this approach, reflecting our labeling efficiency (data not shown). Adult brain microglia remained labeled at this ∼30% rate indicating that yolk sac macrophages labeled at E8.5 persisted faithfully into adulthood. We found that ∼5% of resident cardiac CD11c^{lo} macrophages (both MHC-II^{hi} and MHC-II^{Low}), and Ly6c^{+} macrophages remained labeled in adult mice, while CCR2^{+}CD11c^{+} macrophages were not (Fig 5E). Outside of brain microglia, only the heart and liver retained yolk sac-derived macrophages populations labeled at E8.5, while lung, peritoneal, skin, spleen and kidney macrophages did not (Fig 5E). After normalizing for recombination efficiency, E8.5 labeled yolk sac macrophages that resided within the adult heart and liver comprised ∼15–25% of their respective resident macrophage pools, indicating that yolk-sack macrophage persistence in adult tissue is much more restricted than is currently appreciated. Together, our data suggest that the majority of adult cardiac macrophages developed outside FLT3-dependent pathways and comprised a mixed ontological group containing both embryonic yolk sac-derived macrophages and fetal liver monocyte-derived macrophages. Mice were not born with MHC-II^{hi} macrophages, but rather these macrophages only developed fully by ∼8 weeks of age in a FLT3-independent fashion (Fig S4A), indicating that embryonic MHC-II^{lo} macrophages gave rise to MHC-II^{hi} macrophages after birth.

Definitive HSCs give rise to both *Flt3*-Cre^{-} and *Flt3*-Cre^{+} monocytes

Our data also suggested that the absence of FLT3-mediated recombination defines macrophages that originated during embryonic development, however it may not be able to distinguish between primitive vs. definitive hematopoietic macrophages origins during development. As an example, even in the liver lymphocyte pool at E14.5, only 20% of cells had gone through FLT3 pathways, whereas in the adult, FLT3-driven recombination was typically >95% (Fig S4B). This likely reflects rapid proliferation during embryonic development, resulting in less time spent in a FLT3^{+} intermediate and therefore less efficient recombination (Boyer et al., 2011). To investigate further, definitive fetal liver HSCs from *Flt3*-Cre x *Rosa*-mTmG mice (FLT3-Cre^{-}) were sorted, adoptively transplanted into sublethally irradiated WT mice and gated on engrafted cells. As in the embryo, FLT3-mediated recombination was markedly reduced in monocytes shortly after transplant, however recombination rates increased, and after ∼8 weeks had plateaued (Fig S5A). The engrafted cardiac macrophage subsets that were previously identified to be primarily FLT3-Cre^{-} (Fig 5D, CD11c^{lo} MHC-II^{hi} and MHC-II^{lo}) had reduced recombination rates (Fig S5B). Similarly, lung macrophages also had reduced engraftment rates following irradiation and adoptive transplant (19 ± 6% vs. blood monocytes, $p < 0.01$), and of the engrafted cells, had reduced FLT3-driven recombination, consistent with their fetal-liver monocyte origin (Guilliams et al., 2013). These data suggested that following irradiation, the heart and lung were initially repopulated by FLT3-Cre^{-} blood monocytes that differentiated into long-lasting resident tissue macrophages, since blood monocytes produced at this time had low levels of recombination. There was little replacement of FLT3-Cre^{-} tissue macrophages by FLT3-derived blood monocytes over time, even though they both originated from the same engrafted HSC pool.

If fetal liver monocytes provide a significant source of cardiac tissue macrophages, we hypothesized that the Ly6c^{+} monocyte influx observed after resident macrophage depletion (Fig 2E) would lead to long-term replacement of embryonic (FLT3-independent) monocyte-derived macrophages with adult (FLT3-dependent) monocyte-derived macrophages. To address this, we examined *Flt3-Cre* reporter mice 6 weeks after macrophage depletion and observed replacement of FLT3-Cre^{-} cardiac macrophages with those derived from FLT3-dependent pathways (Fig S5C–S5D). This durable replacement of embryonically derived macrophages with FLT3-dependent adult monocyte-derived macrophages was even more striking in liver and splenic macrophages, while there was no replacement in brain microglia (Fig S5E).

Formal lineage tracing reveal subset specific recruitment and expansion dynamics during inflammation

We next sought to investigate the dynamics of cardiac macrophage populations in the setting of inflammation using an ontological approach to clearly distinguish infiltrating adult blood monocytes from embryonic cardiac macrophages. After AngII infusion, there was expansion of the FLT3-Cre^{-} MHC-II^{lo} macrophage subset and contraction of the FLT3-Cre^{-} MHC-II^{Hi} macrophage subset (Fig 6A–6B), similar to results from experiments using *Ccr*$^{GFP/GFP}$ mice (Fig 4D–4E). There was also an increase in the number of cardiac FLT3-dependent MHC-II^{hi} and MHC-II^{lo} macrophages, indicating expansion from monocytes, derived from adult definitive HSC pathways (Fig 6A–6B). Both FLT3-dependent and independent populations proliferated, thus all macrophages irrespective of their ontological origin had the ability to enter the cell cycle (Fig 6C and 6D).

Monocyte-derived macrophages coordinate cardiac inflammation, while playing redundant but lesser roles in antigen sampling and efferocytosis

To gain functional insight into the distinct populations of cardiac macrophages, we sorted the two main CD11c^{lo}CCR2^{-} macrophage populations (MHC-II^{hi} and MHC-II^{lo}) and CCR2^{+}CD11c^{hi}MHC-II^{hi} macrophages, and compared them to sorted Ly6c^{hi} blood monocytes. Transcriptional profiling revealed ~4500 differentially expressed genes (>2 fold) with large differences between macrophages and blood monocytes, and as expected, smaller differences between each macrophage subset (Fig 7A). Using principle component analysis, each macrophage subset clustered separately (Fig S6A). To determine if cardiac macrophages shared similar genes with other known macrophage populations we compared differentially expressed genes between monocytes and cardiac macrophages in our data set to those differentially expressed genes between monocytes and representative tissue macrophages in the ImmGen Consortium data set (microglia, lung and peritoneal macrophages) (Gautier et al., 2012). We found numerous overlapping and non-overlapping genes across data sets between cardiac macrophages and other tissue macrophage subsets, indicating that cardiac macrophages, like other tissue macrophage populations, possess both common and unique gene expression patterns (Table S2)

Comparing CCR2^{+} macrophages to either of the CCR2^{-} macrophages subsets (MHC-II^{hi} or MHC-II^{lo}) using Gene Ontology revealed enrichment of immune / inflammatory pathways (see Table S3). The primary distinction between CCR2^{-} MHC-II^{hi} and MHC-II^{lo} macrophage subsets was related to antigen processing and presentation. Therefore we focused on the ability of cardiac macrophage subsets to sample antigens. A number of genes involved in endocytosis and intracellular trafficking were differentially expressed (Fig S6B), and there were striking differences in vesicular morphology between the subsets. Compared to Ly6c^{hi}CCR2^{+} blood monocytes, both CD11c^{lo}CCR2^{-} [MHC-II^{hi} and MHC-II^{lo}] macrophages were much larger and contained large cytoplasmic compartments that were not present in monocytes, which was particularly apparent in the CCR2^{-}MHC-II^{lo} population (Fig 7B). We next took several approaches to evaluate uptake and processing of antigens in these cells. First, we found that cardiac macrophages were efficient at rapidly internalizing *i.v.* FITC-dextran in comparison to cardiac DCs and splenic macrophages, and MHC-II^{lo} macrophages were the most efficient cardiac macrophage subset (Fig S6C). To determine if cardiac macrophages internalized molecules or cells from the surrounding microenvironment *in vivo*, we analyzed *Rosa*-TdTom x *Mlc2V*-Cre mice that express the TdTom reporter strictly in cardiomyocytes, and we also observed increased fluorescence in all cardiac macrophage subsets (Fig 7C). This was extended to an *in vitro* system where efferocytosis of labeled apoptotic/necrotic cardiomyocytes was determined. Similar to the results above, cardiac macrophages, and in particular the MHC-II^{lo} macrophage subset, were efficient at taking up dead cell cargo, suggesting that sampling antigen and uptake of local cardiomyocytes (or material from cardiomyocytes) is a common function of cardiac macrophages (Fig 7C & 7D).

MHC-II-expressing cardiac macrophages were enriched for genes involved in antigen presentation suggesting that these cells play a role in immunosurveillance (Fig 7E). To test this hypothesis, sorted cardiac macrophage subsets were either pulsed with peptide or given intact protein (which requires uptake, processing and presentation) and their ability to activate T cells was measured. Both cardiac macrophages subsets that expressed high amounts of MHC-II (CCR2^{-} and CCR2^{+}) were efficient at stimulating T cell responses (whether pulsed with peptide or protein), while MHC-II^{lo} macrophages had only a limited ability to activate T cells, despite their robust ability to take up antigen and cells (Fig 7E). CCR2^{+} macrophages were enriched in genes regulating the Nlrp3 inflammasome (Fig 7F), which is responsible for the release of IL-1β and inflammatory responses in multiple tissues,

including the heart (Mezzaroma et al., 2011). To investigate the role of $CCR2^+$ macrophages in the production of IL-1β *in vivo* after AngII infusion, we quantified cardiac IL-1β protein concentration. As seen in Fig 7F, cardiac IL-1β production was absent in AngII treated $Ccr2^{GFP/GFP}$ mice that lack $CCR2^+$ macrophages. Together, this data reveals overlapping and non-overlapping functions of distinct subsets of resident cardiac macrophages.

Discussion

The long-held belief that blood monocytes give rise to all resident tissue macrophages has been revised by several recent studies. Evidence is emerging that most tissue macrophages populations are established embryonically, persist into adulthood, and turn over through *in situ* proliferation without significant monocyte input in the absence of inflammation (Schulz et al., 2012; Hashimoto et al., 2013; Yona et al., 2013; Hoeffel et al., 2012; Ginhoux et al., 2010). Much less is understood about the precise origin of embryonically established macrophage populations, and their relationship with blood monocytes when homeostasis is disrupted. Here we show that the majority of tissue resident macrophages in adult animals are established embryonically. However, by using fate mapping studies driven by CD115, we refined previous analyses and demonstrated that the heart, liver and brain are the only tissues in which yolk sac-derived macrophages persist into adulthood in substantial numbers. Tissue macrophage populations from the lung, spleen, kidney and skin almost exclusively contain fetal monocytederived macrophages. These tissue macrophages are FLT3-Cre^-, yet they are not derived from embryonic yolk sac macrophages. Rather, our data indicated that tissue macrophages are established at a time when definitive hematopoiesis in the fetal liver inefficiently drove FLT3-dependent recombination, thereby allowing these macrophages to be clearly delineated in adult mice since they were not replaced over the long term by FLT3-dependent blood monocytes (see Fig S7). Transplant of fetal liver definitive $CD150^+$ HSCs revealed that the same progenitor could give rise to both FLT3-Cre^- tissue macrophages and FLT3-dependent blood monocytes. In other words, prior to depletion, embryonically established tissue macrophages are autonomous from blood monocytes. After depletion, and in the setting of competitive resident macrophages proliferation, blood monocyte-derived macrophages have the ability to take up durable residence within tissue and become the dominant macrophages population in some tissues. After repopulation is complete, tissue macrophages autonomy is restored, albeit with a large complement of adult monocyte-derived macrophages as the new resident macrophages population. Our data brings to light the dynamic nature of monocyte / tissue macrophages plasticity within the setting of an ontological framework that is not well appreciated.

After cardiac injury, recruited monocytes and macrophages play a critical role in healing, with either excessive or insufficient expansion in cell numbers clearly linked to pathology (Nahrendorf et al., 2007; Tsujioka et al., 2009; Panizzi et al., 2010). However, our understanding of resident cardiac macrophages populations and their relationship to blood monocytes is lacking. We found that at steady state, the adult mammalian heart contains two separate and discrete cardiac macrophages pools. The first macrophages population ($CCR2^-$, $CD11c^{lo}$) includes the majority of MHC-II^{hi}, MHC-II^{lo}, and $Ly6c^+$ macrophages. These macrophages were separate from the blood monocyte pool and represented an embryonically established lineage made up of progeny from yolk sac macrophages and fetal monocytes. The second macrophages pool was much smaller numerically and was derived from blood $CCR2^+Ly6c^{hi}$ monocytes. Thus, there is more phenotypic heterogeneity amongst cardiac macrophages than previously appreciated (Pinto et al., 2012).

Monocyte and macrophage populations in the heart were also monitored when homeostasis was disrupted. After transient depletion with clodronate liposomes, $Ly6c^{hi}$ monocytes entered the myocardium and were able to differentiate into long lasting populations of

cardiac macrophages. However, proliferation of resident cardiac ($CCR2^{-}$) macrophages also occurred, indicating that local expansion and recruitment both contribute to macrophages repopulation. Our results with cardiac macrophages differ from observations in the lung, in which macrophages are repopulated through expansion of local lung tissue macrophages rather than blood monocyte-dependent recruitment (Hashimoto et al., 2013). These data may reflect tissue differences between macrophage subsets and/or depletion techniques. However, our findings were not restricted to the heart, as a near to complete and durable replacement of embryonic liver and splenic macrophages was observed after depletion. Repopulation after irradiation was more complex, with more similarities between resident cardiac and lung macrophage. Our data reinforced the observation that resident tissue macrophage populations in the heart and lung could compete effectively with adoptively transplanted monocytes, indicating local macrophage expansion in these niches despite genotoxic injury (Hashimoto et al., 2013). Cumulatively, our data strengthen the notion that redundant pathways underlie macrophage repopulation after depletion in multiple tissue beds, and indicate that if expansion by resident embryonic macrophages is insufficient, bone marrow-derived monocyte populations become a viable, alternate, tissue macrophage substitute.

Macrophages are thought to play a critical role in the cardiac remodeling response after damage. After AngII infusion resident cardiac macrophages expanded without peripheral monocyte input through *in situ* proliferation, akin to expansion of pleural macrophages after helminth infection (Jenkins et al., 2011). Infiltrating monocyte-derived macrophages are also able to expand through proliferation, suggesting proliferation may be a key strategy to regulate macrophage density during inflammation (Davies et al., 2013). Prior studies in ischemic myocardium indicated that recruitment, rather than local proliferation, is the primary mechanism regulating monocyte and macrophage numbers (Leuschner et al., 2012). Our data extend these findings and reveal that multiple cardiac macrophage populations that can expand solely through *in situ* proliferation.

All cardiac macrophages subsets were found to sample their environment by internalizing blood borne or local (cardiomyocyte-expressed) antigens. The subsets that expressed high amounts of MHC-II ($CCR2^{+}$ and $CCR2^{-}$ macrophages) efficiently processed and presented antigen to T cells, suggesting a role in immunosurveillance. Alternatively, resident cardiac macrophages, in particular the MHC-II^{Low} subset, are capable of phagocytosing dying cardiomyocytes, thereby contributing to local homeostatic processes. After myocardial injury, inflammasome activation leads to poor tissue regeneration, while blockade of the CCR2 axis prevents ischemic injury (Mezzaroma et al., 2011; Frangogiannis et al., 2007). We observed that numerous genes involved in IL-1β production via the NLPR3 inflammasome were differentially expressed in $CCR2^{+}$ macrophages, and confirmed that IL-1β production in the setting of *in vivo* cardiac stress was dependent on expansion of $CCR2^{+}$ monocytes and macrophages. Our data may explain why, in models of cardiac injury, blocking monocyte influx (and thereby subsequent $CCR2^{+}$ macrophages expansion) is protective, whereas broad macrophage depletion strategies that also target resident $CCR2^{-}$ cardiac macrophage abolish protection (van Amerongen et al., 2007; Kaikita et al., 2004). Together, these data suggest that preserving resident cardiac macrophages expansion via proliferation, while targeting peripheral monocyte recruitment may lead to improved myocardial recovery after injury.

In summary, here we showed that the adult mammalian myocardium contains diverse macrophages populations with distinct ontological origins. We also defined the role of local proliferation and blood monocyte recruitment to the maintenance of these populations at steady state and in response to stress. Our data also provide a genetic framework for understanding the role of cardiac macrophage biology in health and disease, which may

facilitate further mechanistic and/or therapeutic studies to identify subset-specific pathways that contribute to end-organ damage, while leaving cytoprotective pathways intact.

Experimental Procedures

Mice, tissue isolation and flow cytometry

The mouse strains utilized in this study are described in detail within the supplemental experimental procedures. Prior to organ collection, mice were sacrificed and perfused with cold phosphate-buffered saline, tissues were minced, digested and processed into single cells suspensions as previously described (Nahrendorf et al., 2007) with modifications (see supplemental Experimental procedures). Detailed gating strategies, antibodies used and sorting strategies can be found in the supplemental experimental procedures.

Osmotic mini-pump implantation, myocardial infarction surgery and parabiosis

Mice with anesthetized with ketamine/xylazine, the back was shaved and mini pumps (Alzet) containing either saline or angiotensin II (AngII) (Bachem, 1.5 – 2.0 mg/kg/day) were implanted. The incisions were closed with silk sutures. Complete left anterior descending artery occlusion was performed as previously described (Sondergaard et al., 2010). C57BL/6J and B6-Ly5.1 female mice controlled for age and weight were parabiosed as described (Peng et al., 2013).

Transcriptional array

Cardiac macrophages (three populations) and Ly6c^{hi} blood monocytes were sorted directly into trizol and the RNA was extracted (Qiagen). 1 ng of total RNA was amplified, labeled cDNAs were hybridized to Agilent Mouse 4×44K V2 microarrays. See supplemental experimental procedures for additional details.

Cardiomyocyte phagocytosis and antigen presentation assays

Macrophage-mediated uptake of dying cardiomyocytes was performed as previously described (Mounier et al., 2013). Cardiac single cell suspensions or splenocytes from *Ccr2*$^{GFP/+}$ mice were labeled with cell-surface antibodies and incubated with apoptotic and necrotic cardiomyocytes (at either 4°C or 37°C) in order to distinguish surface binding (4°C) from active phagocytosis (37°C). To assess antigen presentation ability, sorted cardiac macrophages and Ly-6c^{Hi} monocytes were plated and incubated with either Listeriolysin O (LLO) peptide or LLO protein as previously described (Carrero et al., 2012). A T cell hybridoma specific for LLO was then added and IL-2 production assessed. See supplemental experimental procedures for additional details.

Supplementary Material

Refer to Web version on PubMed Central for supplementary material.

Acknowledgments

Funding for these studies was provided by AHA-SDG-12SDG8030003 (SE), NIH K08HL112826-01 (SE) and T32HL007081-37 (SE, KJL), T32CA009547 (DKS) and RO1 HL111094-02 (DLM). We thank Ms. Liping Yang for experimental help and advice on parabiosis, Ms. Joan Avery and Mrs. Kassandra Weber for their technical assistance, and Ms. Susan Gilfillan for generating the *Ccr2*$^{GFP/GFP}$. This work benefitted from data assembled by the ImmGen consortium.

References

Boyer SW, Schroeder AV, Smith-Berdan S, Forsberg EC. All hematopoietic cells develop from hematopoietic stem cells through Flk2/Flt3-positive progenitor cells. Cell Stem Cell. 2011; 9:64–73. [PubMed: 21726834]

Carrero JA, Vivanco-Cid H, Unanue ER. Listeriolysin o is strongly immunogenic independently of its cytotoxic activity. PLoS. One. 2012; 7:e32310. [PubMed: 22403645]

Davies LC, Rosas M, Jenkins SJ, Liao CT, Scurr MJ, Brombacher F, Fraser DJ, Allen JE, Jones SA, Taylor PR. Distinct bone marrow-derived and tissue-resident macrophage lineages proliferate at key stages during inflammation. Nat. Commun. 2013; 4:1886. [PubMed: 23695680]

Francis GS. Neurohormonal control of heart failure. Cleve. Clin. J. Med. 2011; 78(Suppl):S75–S79. [PubMed: 21972336]

Frangogiannis NG, Dewald O, Xia Y, Ren G, Haudek S, Leucker T, Kraemer D, Taffet G, Rollins BJ, Entman ML. Critical role of monocyte chemoattractant protein-1/CC chemokine ligand 2 in the pathogenesis of ischemic cardiomyopathy. Circulation. 2007; 115:584–592. [PubMed: 17283277]

Gautier EL, Shay T, Miller J, Greter M, Jakubzick C, Ivanov S, Helft J, Chow A, Elpek KG, Gordonov S, Mazloom AR, Ma'ayan A, Chua WJ, Hansen TH, Turley SJ, Merad M, Randolph GJ. Gene-expression profiles and transcriptional regulatory pathways that underlie the identity and diversity of mouse tissue macrophages. Nat. Immunol. 2012; 13:1118–1128. [PubMed: 23023392]

Ginhoux F, Greter M, Leboeuf M, Nandi S, See P, Gokhan S, Mehler MF, Conway SJ, Ng LG, Stanley ER, Samokhvalov IM, Merad M. Fate mapping analysis reveals that adult microglia derive from primitive macrophages. Science. 2010; 330:841–845. [PubMed: 20966214]

Guilliams M, De KI, Henri S, Post S, Vanhoutte L, De PS, Deswarte K, Malissen B, Hammad H, Lambrecht BN. Alveolar macrophages develop from fetal monocytes that differentiate into long-lived cells in the first week of life via GM-CSF. J. Exp. Med. 2013

Hashimoto D, Chow A, Noizat C, Teo P, Beasley MB, Leboeuf M, Becker CD, See P, Price J, Lucas D, Greter M, Mortha A, Boyer SW, Forsberg EC, Tanaka M, van RN, Garcia-Sastre A, Stanley ER, Ginhoux F, Frenette PS, Merad M. Tissue-Resident Macrophages Self-Maintain Locally throughout Adult Life with Minimal Contribution from Circulating Monocytes. Immunity. 2013; 38:792–804. [PubMed: 23601688]

Hashimoto D, Miller J, Merad M. Dendritic cell and macrophage heterogeneity in vivo. Immunity. 2011; 35:323–335. [PubMed: 21943488]

Hoeffel G, Wang Y, Greter M, See P, Teo P, Malleret B, Leboeuf M, Low D, Oller G, Almeida F, Choy SH, Grisotto M, Renia L, Conway SJ, Stanley ER, Chan JK, Ng LG, Samokhvalov IM, Merad M, Ginhoux F. Adult Langerhans cells derive predominantly from embryonic fetal liver monocytes with a minor contribution of yolk sac-derived macrophages. J. Exp. Med. 2012; 209:1167–1181. [PubMed: 22565823]

Jenkins SJ, Ruckerl D, Cook PC, Jones LH, Finkelman FD, van RN, MacDonald AS, Allen JE. Local macrophage proliferation, rather than recruitment from the blood, is a signature of TH2 inflammation. Science. 2011; 332:1284–1288. [PubMed: 21566158]

Kaikita K, Hayasaki T, Okuma T, Kuziel WA, Ogawa H, Takeya M. Targeted deletion of CC chemokine receptor 2 attenuates left ventricular remodeling after experimental myocardial infarction. Am. J. Pathol. 2004; 165:439–447. [PubMed: 15277218]

Kumaravelu P, Hook L, Morrison AM, Ure J, Zhao S, Zuyev S, Ansell J, Medvinsky A. Quantitative developmental anatomy of definitive haematopoietic stem cells/long-term repopulating units (HSC/RUs): role of the aorta-gonad-mesonephros (AGM) region and the yolk sac in colonisation of the mouse embryonic liver. Development. 2002; 129:4891–4899. [PubMed: 12397098]

Leuschner F, Rauch PJ, Ueno T, Gorbatov R, Marinelli B, Lee WW, Dutta P, Wei Y, Robbins C, Iwamoto Y, Sena B, Chudnovskiy A, Panizzi P, Keliher E, Higgins JM, Libby P, Moskowitz MA, Pittet MJ, Swirski FK, Weissleder R, Nahrendorf M. Rapid monocyte kinetics in acute myocardial infarction are sustained by extramedullary monocytopoiesis. J. Exp. Med. 2012; 209:123–137. [PubMed: 22213805]

Lichanska AM, Hume DA. Origins and functions of phagocytes in the embryo. Exp. Hematol. 2000; 28:601–611. [PubMed: 10880746]

Mezzaroma E, Toldo S, Farkas D, Seropian IM, Van Tassell BW, Salloum FN, Kannan HR, Menna AC, Voelkel NF, Abbate A. The inflammasome promotes adverse cardiac remodeling following acute myocardial infarction in the mouse. Proc. Natl. Acad. Sci. U. S. A. 2011; 108:19725–19730. [PubMed: 22106299]

Mounier R, Theret M, Arnold L, Cuvellier S, Bultot L, Goransson O, Sanz N, Ferry A, Sakamoto K, Foretz M, Viollet B, Chazaud B. AMPKalpha1 regulates macrophage skewing at the time of resolution of inflammation during skeletal muscle regeneration. Cell Metab. 2013; 18:251–264. [PubMed: 23931756]

Nahrendorf M, Swirski FK, Aikawa E, Stangenberg L, Wurdinger T, Figueiredo JL, Libby P, Weissleder R, Pittet MJ. The healing myocardium sequentially mobilizes two monocyte subsets with divergent and complementary functions. J. Exp. Med. 2007; 204:3037–3047. [PubMed: 18025128]

Panizzi P, Swirski FK, Figueiredo JL, Waterman P, Sosnovik DE, Aikawa E, Libby P, Pittet M, Weissleder R, Nahrendorf M. Impaired infarct healing in atherosclerotic mice with Ly-6C(hi) monocytosis. J. Am. Coll. Cardiol. 2010; 55:1629–1638. [PubMed: 20378083]

Peng H, Jiang X, Chen Y, Sojka DK, Wei H, Gao X, Sun R, Yokoyama WM, Tian Z. Liver-resident NK cells confer adaptive immunity in skin-contact inflammation. J. Clin. Invest. 2013; 123:1444–1456. [PubMed: 23524967]

Pinto AR, Paolicelli R, Salimova E, Gospocic J, Slonimsky E, Bilbao-Cortes D, Godwin JW, Rosenthal NA. An abundant tissue macrophage population in the adult murine heart with a distinct alternatively-activated macrophage profile. PLoS. One. 2012; 7:e36814. [PubMed: 22590615]

Qian BZ, Li J, Zhang H, Kitamura T, Zhang J, Campion LR, Kaiser EA, Snyder LA, Pollard JW. CCL2 recruits inflammatory monocytes to facilitate breast-tumour metastasis. Nature. 2011; 475:222–225. [PubMed: 21654748]

Satpathy AT, KC W, Albring JC, Edelson BT, Kretzer NM, Bhattacharya D, Murphy TL, Murphy KM. Zbtb46 expression distinguishes classical dendritic cells and their committed progenitors from other immune lineages. J. Exp. Med. 2012; 209:1135–1152. [PubMed: 22615127]

Schulz C, Gomez PE, Chorro L, Szabo-Rogers H, Cagnard N, Kierdorf K, Prinz M, Wu B, Jacobsen SE, Pollard JW, Frampton J, Liu KJ, Geissmann F. A lineage of myeloid cells independent of Myb and hematopoietic stem cells. Science. 2012; 336:86–90. [PubMed: 22442384]

Serbina NV, Pamer EG. Monocyte emigration from bone marrow during bacterial infection requires signals mediated by chemokine receptor CCR2. Nat. Immunol. 2006; 7:311–317. [PubMed: 16462739]

Sondergaard CS, Hess DA, Maxwell DJ, Weinheimer C, Rosova I, Creer MH, Piwnica-Worms D, Kovacs A, Pedersen L, Nolta JA. Human cord blood progenitors with high aldehyde dehydrogenase activity improve vascular density in a model of acute myocardial infarction. J. Transl. Med. 2010; 8:24. [PubMed: 20214792]

Tacke F, Ginhoux F, Jakubzick C, van RN, Merad M, Randolph GJ. Immature monocytes acquire antigens from other cells in the bone marrow and present them to T cells after maturing in the periphery. J. Exp. Med. 2006; 203:583–597. [PubMed: 16492803]

Tagliani E, Shi C, Nancy P, Tay CS, Pamer EG, Erlebacher A. Coordinate regulation of tissue macrophage and dendritic cell population dynamics by CSF-1. J. Exp. Med. 2011; 208:1901–1916. [PubMed: 21825019]

Tsujioka H, Imanishi T, Ikejima H, Kuroi A, Takarada S, Tanimoto T, Kitabata H, Okochi K, Arita Y, Ishibashi K, Komukai K, Kataiwa H, Nakamura N, Hirata K, Tanaka A, Akasaka T. Impact of heterogeneity of human peripheral blood monocyte subsets on myocardial salvage in patients with primary acute myocardial infarction. J. Am. Coll. Cardiol. 2009; 54:130–138. [PubMed: 19573729]

van Amerongen MJ, Harmsen MC, van Rooijen N, Petersen AH, van Luyn MJ. Macrophage depletion impairs wound healing and increases left ventricular remodeling after myocardial injury in mice. Am. J. Pathol. 2007; 170:818–829. [PubMed: 17322368]

Yona S, Kim KW, Wolf Y, Mildner A, Varol D, Breker M, Strauss-Ayali D, Viukov S, Guilliams M, Misharin A, Hume DA, Perlman H, Malissen B, Zelzer E, Jung S. Fate Mapping Reveals Origins and Dynamics of Monocytes and Tissue Macrophages under Homeostasis. Immunity. 2013; 38:79–91. [PubMed: 23273845]

Zhu SN, Chen M, Jongstra-Bilen J, Cybulsky MI. GM-CSF regulates intimal cell proliferation in nascent atherosclerotic lesions. J. Exp. Med. 2009; 206:2141–2149. [PubMed: 19752185]

Zigmond E, Varol C, Farache J, Elmaliah E, Satpathy AT, Friedlander G, Mack M, Shpigel N, Boneca IG, Murphy KM, Shakhar G, Halpern Z, Jung S. Ly6C hi monocytes in the inflamed colon give rise to proinflammatory effector cells and migratory antigen-presenting cells. Immunity. 2012; 37:1076–1090. [PubMed: 23219392]

Highlights

- Yolk sac & fetal monocyte progenitors give rise to adult cardiac macrophages
- Yolk sac macrophages persisted into adulthood only in the heart, liver & brain
- Embryonically established resident macrophages can be replaced by blood monocytes
- Cardiac macrophages differentially activate T cells & take up dying cardiomyocytes

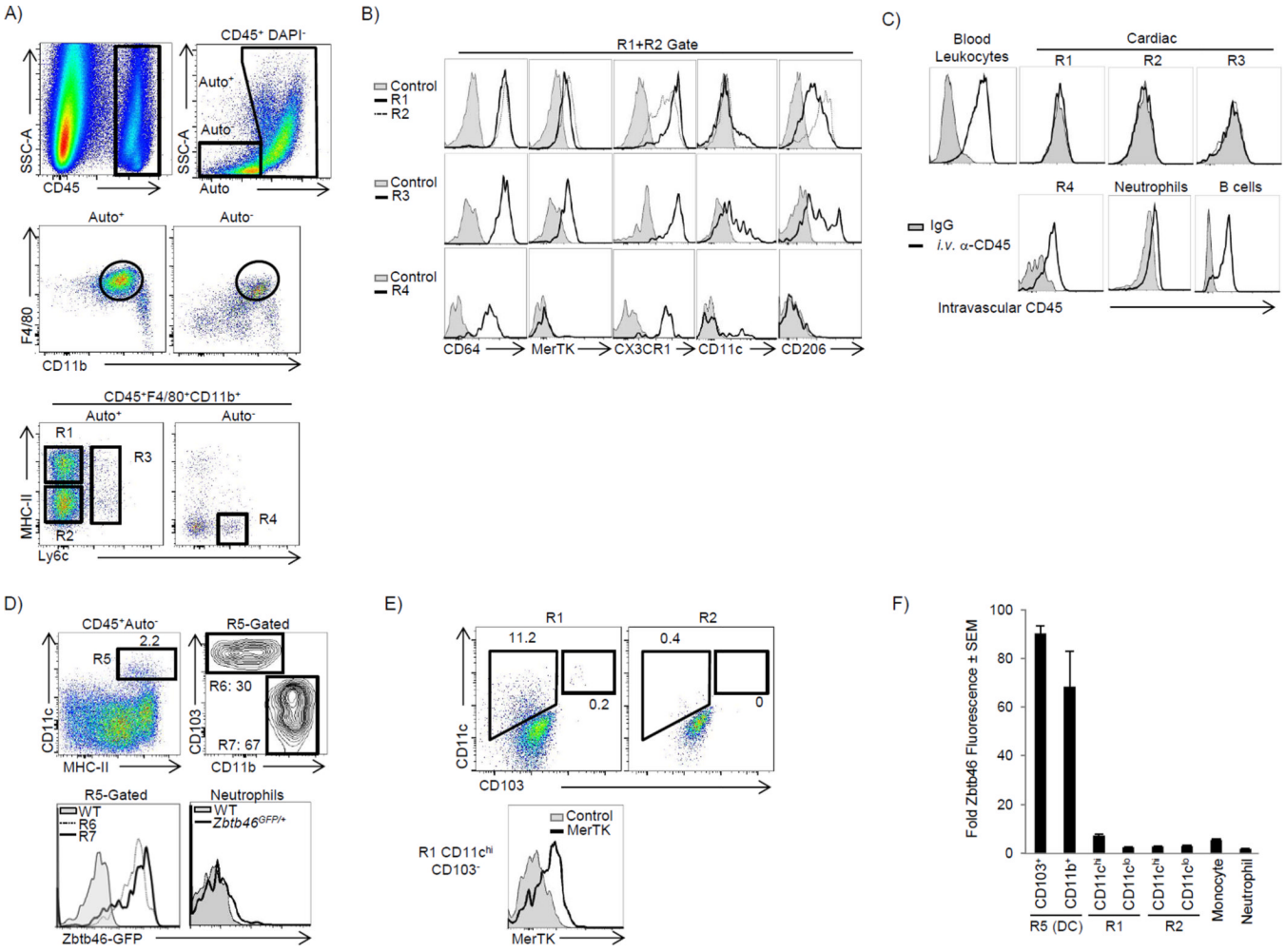

Figure 1. The adult heart contains distinct cardiac macrophage subsets (see also Fig S1)

Cardiac single cell suspensions were analyzed by flow cytometry – see full gating strategy in Fig S1A. A) $CD45^+$ leukocytes were identified, doublets excluded (by FSC-W vs. FSC-A) and dead cells excluded by DAPI. Live cells were stratified by autofluorescence ($Auto^+$ or $Auto^-$), gated on $F4/80^+$ $CD11b^+$ myeloid cells and further stratified by MHC-II and Ly6c expression. R1: MHC-II^{hi} macrophages. R2: MHC-II^{lo} macrophages. R3: $Ly6c^+$ macrophages. R4: $Ly6c^{hi}$ monocytes. B) Cardiac samples were labeled with isotype control antibody (Control) or with the indicated antibodies. Expression of CX3CR1 was assessed in *Cx3cr1*$^{GFP/+}$ mice and compared with WT mice (Control). C) To label intravascular leukocytes, mice were injected *i.v.* with anti-CD45 and sacrificed 5 min later. Cells were gated as in panel A and intravascular CD45 fluorescence is shown. B cells were $B220^+$ $MHCII^+$ $CD11b^-F4/80^-$ and neutrophils were $Ly6g^+$ $CD11b^+$ $F4/80^-$. D) The $Auto^-$ subset contained the majority of cardiac DCs (Total DCs - R5), which were made up of $CD103^+$ $CD11b^-$ (R6) and $CD103^-CD11b^{Hi}$ (R7) DCs. ZBTB46 expression was assessed in *Zbtb46*$^{GFP/+}$ mice in R6 and R7, and compared to $Ly6g^+$ neutrophils and compared to WT mice. E) Expression of CD11c and CD103 within the primary macrophage gates (R1 and R2). F) Relative Zbtb46 fluorescence ratio in myeloid subsets within the myocardium. The geometric mean fluorescence intensity (gMFI) in each subset in *Zbtb46*$^{GFP/+}$ mice was divided by gMFI of that subset in WT mice. The primary macrophages populations in R1 and R2 were further stratified by CD11c expression. N=4–8.

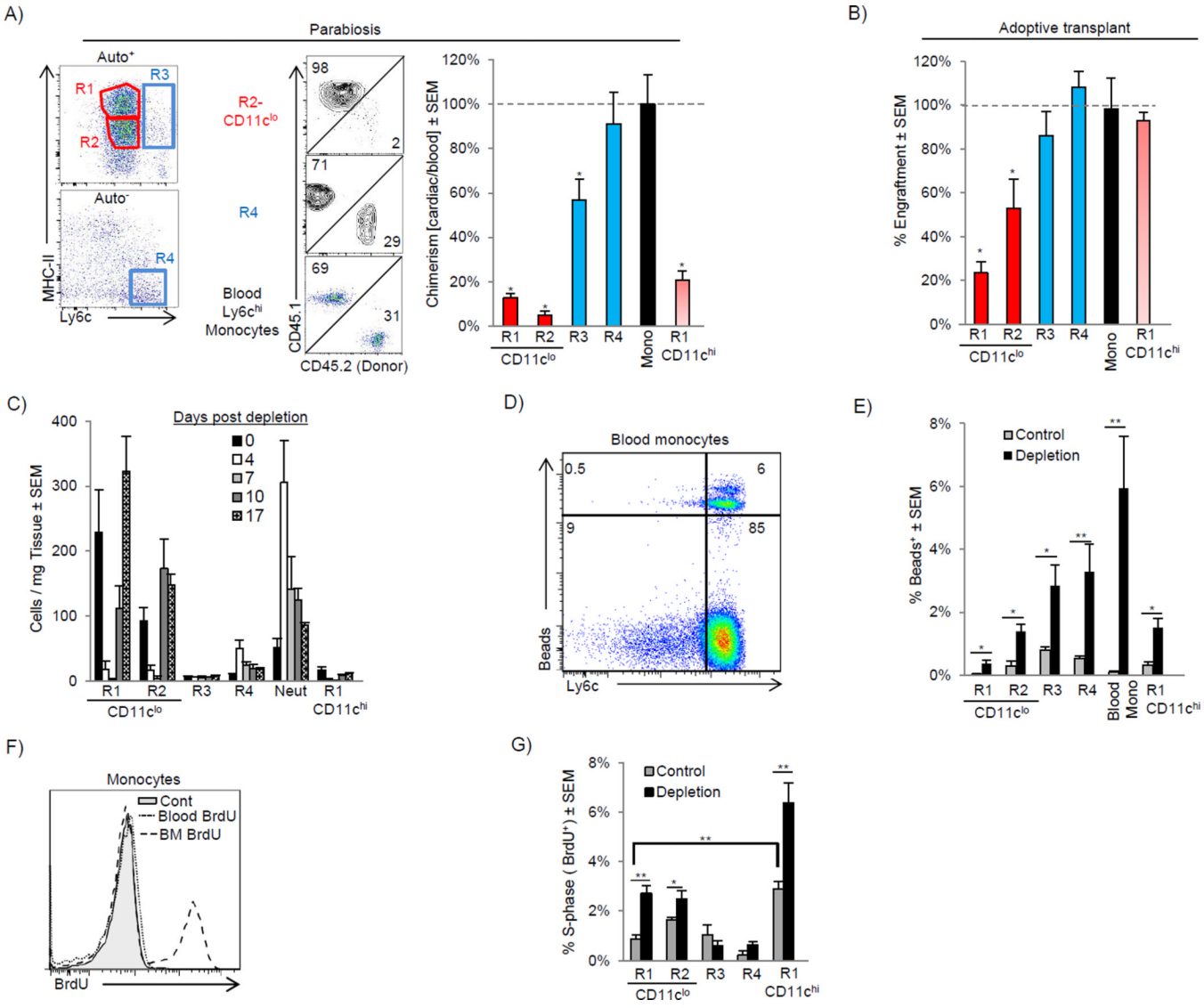

Figure 2. Distinct mechanisms regulate cardiac macrophage turnover in steady and following the disruption of homeostasis

A) CD45.1 and CD45.2 mice were surgically joined to create parabiotic mice and were analyzed after 2 weeks. Dot plots show rate of chimerism for representative populations. The percentage chimerism for each cardiac monocyte and macrophage subset was normalized for the chimeric rate for blood monocytes and expressed as a percentage. B) E14.5 Fetal liver CD150^{+} HSCs were sorted and adoptively transplanted into sublethally irradiated mice. 16 weeks after transplant, mice were harvested and engraftment of transplanted cells was assessed in blood monocytes and cardiac monocytes and macrophage populations. Engraftment for cardiac populations was normalized for blood monocyte engraftment. C–G) Mice were injected with either control liposomes (Control) or liposomes containing clodronate to deplete cardiac macrophages (Depletion) and analyzed over time (C). D–E) Ly6c^{Hi} blood monocytes were labeled with fluorescent microspheres *in vivo* after macrophage depletion (Tacke et al., 2006). D) Bead expression in SSC^{Low}CD115^{+}F4/80^{+} blood monocytes after macrophage depletion. E) Percentage of cardiac bead^{+} cells after depletion. F) To assess proliferation, mice were injected with BrdU and analyzed 2 hrs post injection. Proliferation (BrdU^{+}) in Ly6c^{hi} monocytes in the bone marrow (BM) and blood is

shown. G) Percentage of proliferating $BrdU^+$ cells following macrophage depletion (7 days) within the myocardium in each subset. N=4–7, * P <0.05. ** P<0.01. Data represents at least two experiments, n= 6–12 mice per group.

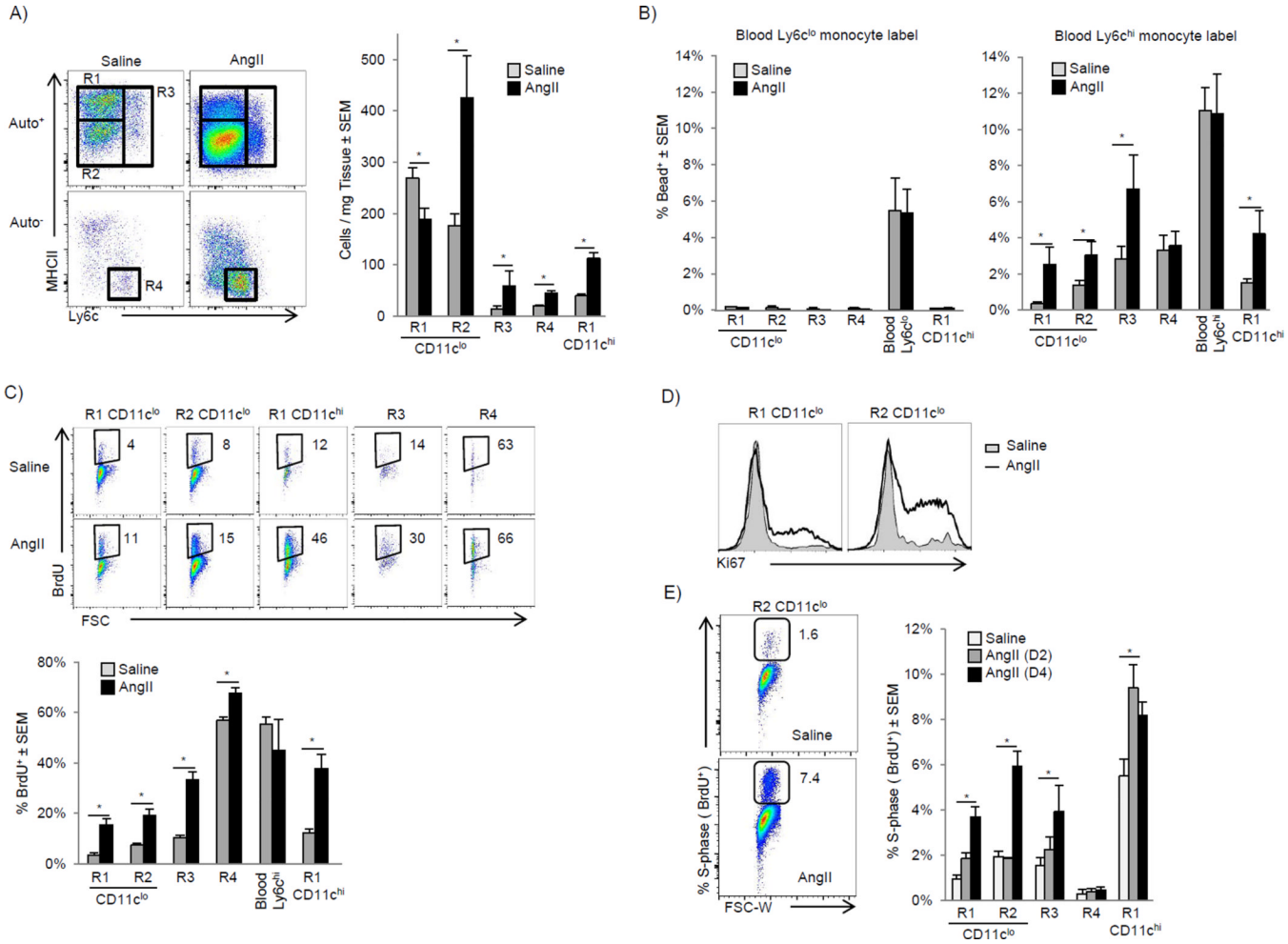

Figure 3. AngII infusion induces numerical expansion of cardiac macrophage through monocytes recruitment and local proliferation (see also Fig S2)

A–E). WT mice were implanted with pumps containing either saline or AngII (2 mg/kg/day). A) Flow cytometric profiles 4 days post infusion gated as in Fig 1A, and graphed numerically. B) Mice with *in vivo* bead-labeled Ly6c^{lo} or Ly6c^{hi} monocytes were implanted with pumps as above, blood and cardiac tissue was analyzed on day 4 and the percentage of bead^{+} cells is shown. C) Osmotic pumps containing either saline or AngII (2 mg/kg/day) were implanted and Ly6c^{hi} monocytes were labeled by injecting mice with BrdU 48 and 24 hrs prior to harvest. Mice were sacrificed 3 days after pump implantation and BrdU detected by flow cytometry. D) Intracellular Ki-67 was detected by flow cytometry 4 days after pump implantation as Fig 3A. E) Percentage of proliferating cells in s-phase was assessed by a single BrdU pulse 2 hrs prior to harvest. Mice were sacrificed 2 or 4 days after pump implantation. Representative flow cytometric profiles at day 4 in MHC-II^{lo} CD11c^{lo} macrophages (R2) and the percentage of BrdU^{+} cells in each gate. * P<0.05. 2–4 independent experiments, 4–7 mice per group.

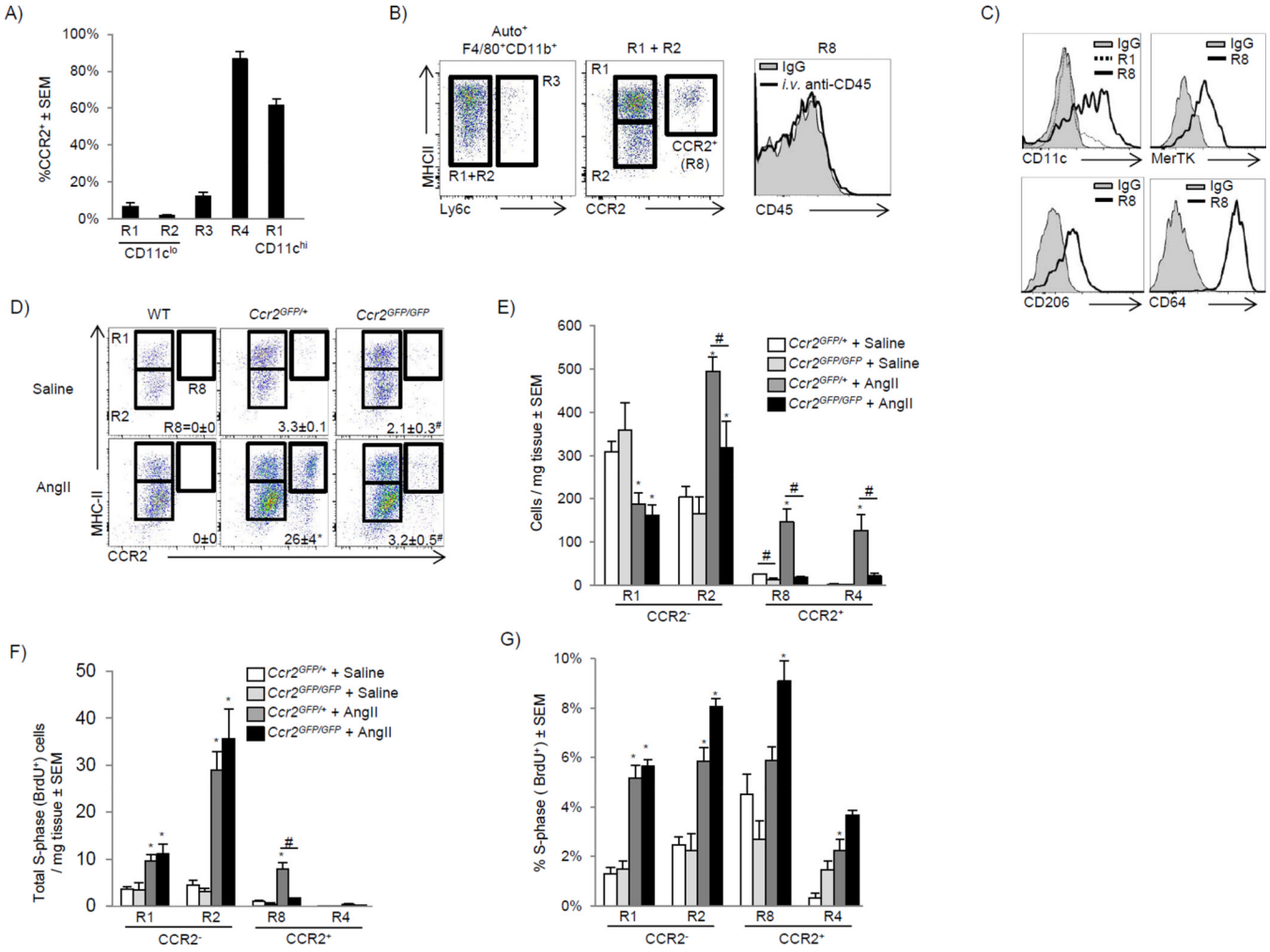

Figure 4. CCR2 deficient mice distinguish local macrophage expansion from influx of peripheral monocytes (see also Fig S3)

A) Cardiac single cell suspensions from *Ccr2*$^{GFP/+}$mice were gated as in Fig 1A and percentage of CCR2^{+} cells in each gate is shown. B) Ly6c MHC-II^{hi} and MHC-II^{lo} macrophages were gated together (R1+R2) in order identify CCR2^{+} macrophages (R8). To determine if CCR2^{+} macrophages were extravascular, mice were injected with anti-CD45 *i.v.* as in Fig 1C and intravascular CD45 expression is shown. C) Expression of CD11c, MerTK, CD206 and CD64 was assessed in the regions as outlined. D–G) Either saline or AngII (1.5 mg/kg/day) containing pumps were implanted and cardiac tissue analyzed at day 4 in either *Ccr2*$^{GFP/+}$ or *Ccr2*$^{GFP/GFP}$ mice. D) Cells were gated as in Fig 4B and the percentage of CCR2^{+} macrophages (R8) is given. E) Total cell numbers, including gating on cardiac Auto^{-} Ly6c^{+}CCR2^{+} monocytes (R4). F) Total number of proliferating cells (BrdU^{+}, S-phase) per mg of tissue after a 2 hr BrdU pulse, and G) the percentage of cells in S-phase in each subset. 2–4 independent experiments, 4–8 mice per group. * P<0.05 vs. saline, $^{\#}$ P<0.05 vs. *Ccr2*$^{GFP/+}$.

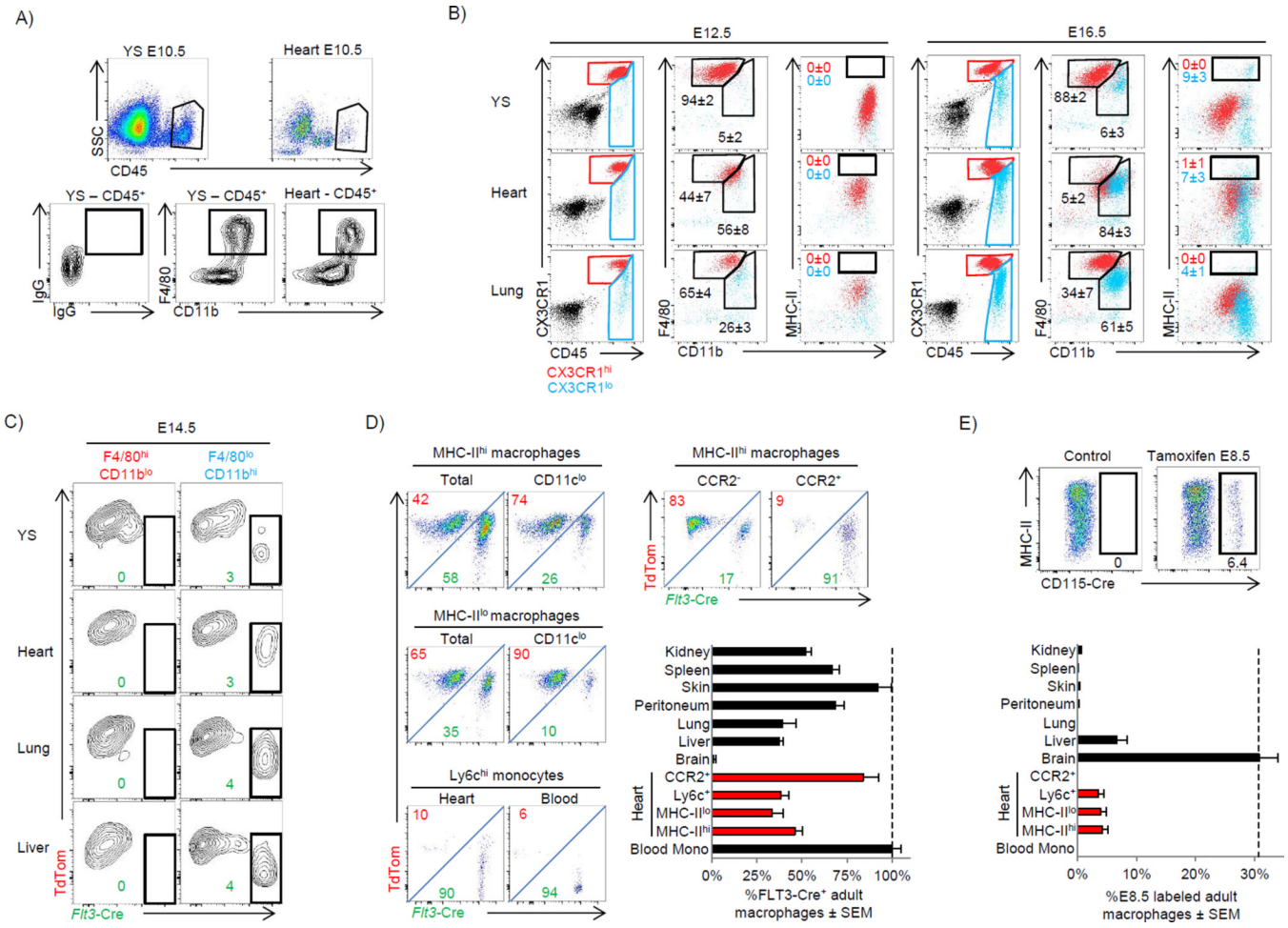

Figure 5. Prenatal macrophages colonize the embryonic heart and persist into adulthood (see also Fig S4 and S5)

A–B) *Cx3cr1*$^{GFP/+}$ embryos were extracted from pregnant females at either E10.5, E12.5 or E16.5. A) Comparison of macrophage populations between the yolk sac (YS) and heart tissue at E10.5. Red color indicates CD45^{+}CX3CR1^{hi} and blue indicates CD45^{+}CX3CR1^{lo} cells. B) Comparison of yolk sac, heart and lung macrophages at E12.5 and E16.5. C) *Flt3*-Cre *Rosa*-mTmG mice were analyzed for reporter expression (E14.5) in embryonic macrophages from various tissues. 2–4 litters for each time point with pooled tissue from 2–6 embryos per animal were used. D) Flow plots showing of adult cardiac macrophages populations in *Flt3*-Cre *Rosa*-mTmG mice. Graphed data represent FLT3-derived cardiac macrophages subsets (red), and other tissue macrophages. Data was normalized to blood monocyte FLT3 recombination, which was typically ~90%. MHC-II^{Hi} and MHC-II^{Low} macrophages were gated on the CD11c^{lo} subsets as in Fig 2A. CCR2^{+} macrophages (R8) were gated as in Fig 4B. E) *CD115-Mer-iCre-Mer Rosa*-mTmG mice were gavaged with tamoxifen at E8.5 to label the progeny of yolk sac macrophages. Mice were sacrificed at 10 weeks of age to determine whether yolk sac macrophage progeny persisted into adulthood. Cardiac macrophages were gated on CD45^{+} Auto^{+} F4/80^{+} CD11b^{+} Ly6c^{-} CD11c^{lo} resident macrophage subsets. Graphed data represent yolk sac-derived cardiac macrophage subsets (red), and other tissue macrophages. See supplemental methods for exact gating strategies for each tissue macrophage population. Experiments were repeated at least twice, n=4–8 animals were group.

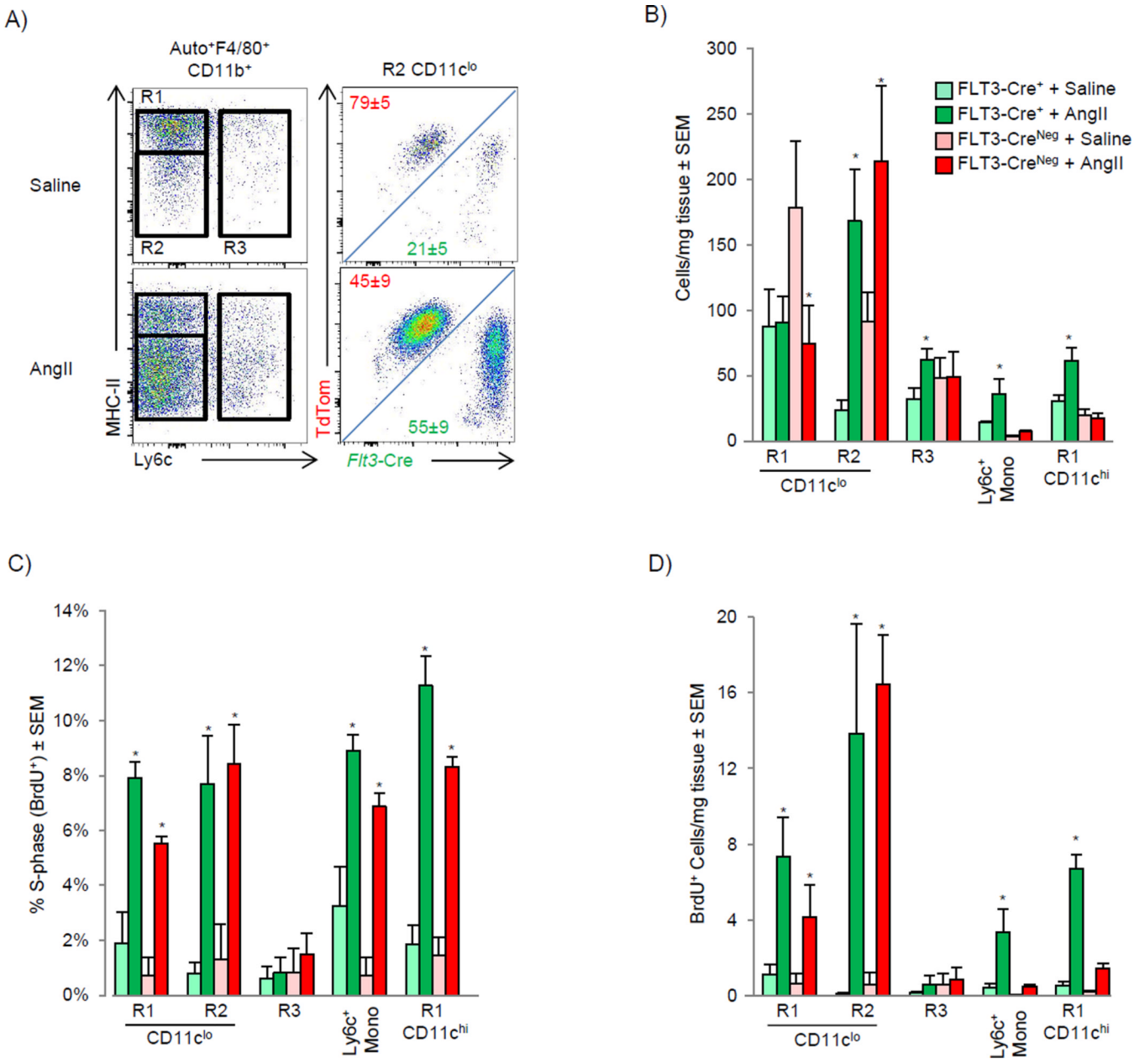

Figure 6. Genetic lineage tracing during AngII induced inflammation

A–D) *FLT3*-Cre *x Rosa* mTmG mice were analyzed for reporter expression in the myocardium and blood in mice implanted with either saline or AngII containing pumps for 4 days (2 mg/kg/day). A) Representative flow cytometric plots from MHC-II^{lo}CD11c^{lo} macrophages and cumulative total cells counts per mg of tissue (B) in each lineage (FLT3-Cre^{+}: Green, FLT3-Cre^{-}: Red). C–D) *Flt3*-Cre *x Rosa* mTmG mice were pulsed with BrdU 2 hrs prior to harvest. C) Percentage of cells in S-phase, and D) Total number of cells in S-phase in each subset is shown. Experiments were repeated at least twice, n=4–6 animals were group. * P<0.05 vs. saline.

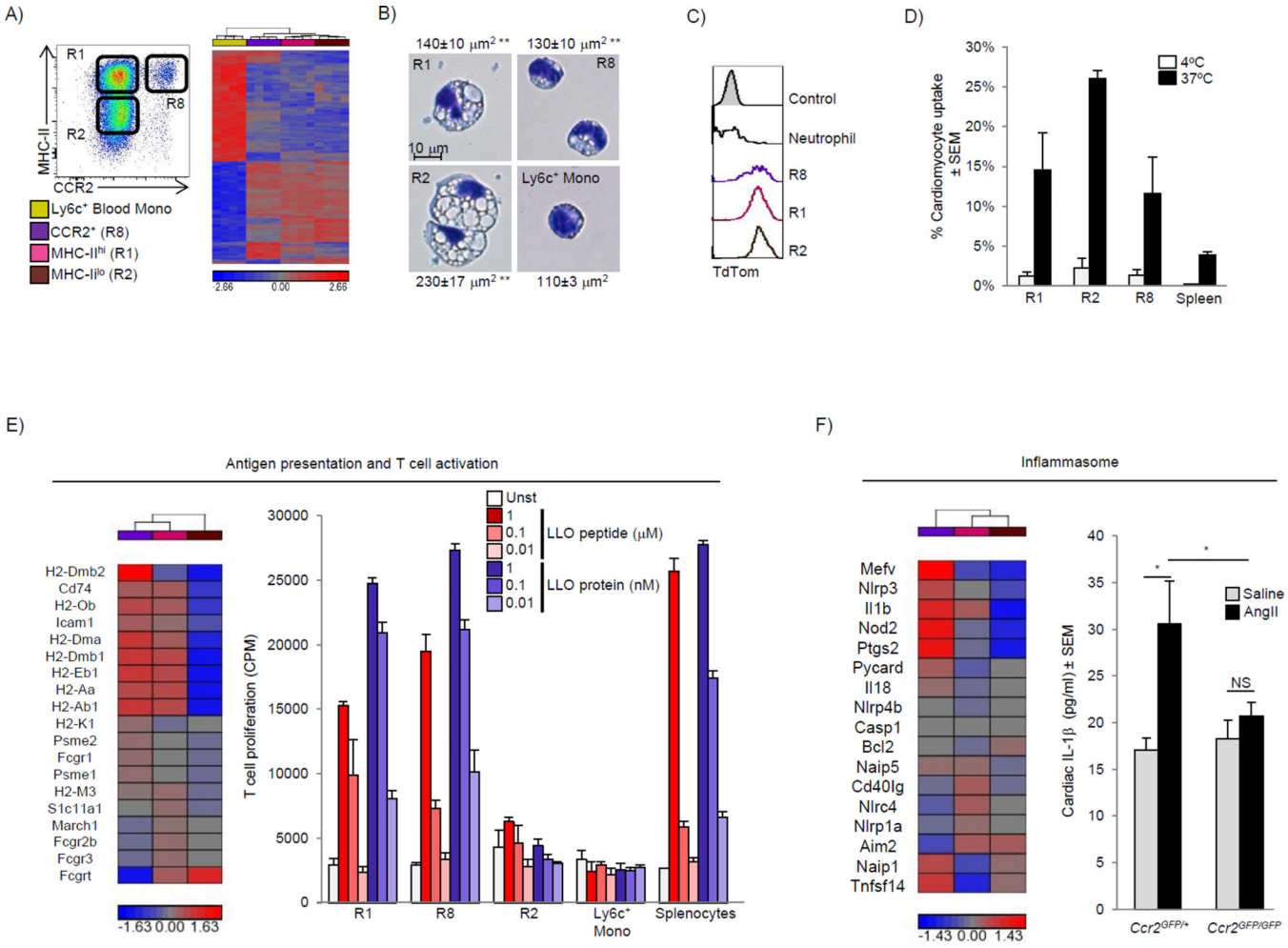

Figure 7. Adult-derived macrophages coordinate cardiac inflammation, while playing redundant but lesser roles in antigen sampling and efferocytosis (see also Fig S6, Table S2 and S3)

Blood Ly6c^{hi} monocytes (yellow), MHC-II^{hi} CCR2^{-} macrophages (R1, Pink) MHC-II^{lo} CCR2^{-} macrophage (R2, brown) and CCR2^{+} MHC-II^{hi} macrophages (R8, purple) were sorted from *Ccr2*$^{GFP/+}$ mice (4 replicates), RNA was extracted and global transcriptional profiling performed. A) Hierarchal clustering of 4557 genes differentially expressed in the entire cell population (Fold change >2). B) Sorted macrophage and Ly6c^{hi} blood monocyte subsets were stained with Hema3 solution, surface area was calculated based on an average of at least 20 cells, ** P<0.01 vs. Ly6c^{+} monocytes. C) Expression of TdTom was determined in cardiac macrophages and neutrophils (Ly6g^{+}CD11b^{+}F4/80^{-}) from cardiomyocyte restricted reporter mice (*Mlc2V*-Cre *x Rosa*-TdTom). Control represents background cardiac macrophage fluorescence from WT mice. D) Fluorescently labeled apoptotic / necrotic cardiomyocytes from WT mice were incubated with cardiac (or splenic) single cell suspension from *Ccr2*$^{GFP/+}$ mice for 4 hours, at either 4°C or 37°C to assess phagocytic uptake. The percentage of macrophage that took up labeled cardiomyocytes was determined by flow cytometry. E) Hierarchical clustering of genes regulating antigen processing and presentation in cardiac macrophages. Sorted cardiac macrophages (as in Fig 7A) were incubated with either Listeriolysin O (LLO) peptide (190–201), or LLO protein (WW non-hemolytic variant), and T cell activation was assessed by IL-2 driven H^{3} thymidine uptake and expressed in counts per minute (see experimental procedures). F) Hierarchical clustering of genes regulating inflammasome activation in cardiac

macrophages. *In vivo* cardiac IL-1β production was measured in cardiac tissue lysate from mice (*Ccr2*$^{GFP/+}$ or *Ccr2*$^{GFP/GFP}$) infused with either saline or AngII (2 mg/kg/day) for 4 days. Each experiment was repeated at least twice, with 2–6 mice / group. * $P<0.05$.